



HAL
open science

Electron transport pathways in isolated chromoplasts from *Narcissus pseudonarcissus* L

Magda Grabsztunowicz, Paula Mulo, Frauke Baymann, Risa Mutoh, Genji Kurisu, Pierre Sétif, Peter Beyer, Anja Krieger-Liszkay

► **To cite this version:**

Magda Grabsztunowicz, Paula Mulo, Frauke Baymann, Risa Mutoh, Genji Kurisu, et al.. Electron transport pathways in isolated chromoplasts from *Narcissus pseudonarcissus* L. *Plant Journal*, 2019, 10.1111/tpj.14319 . hal-02397878

HAL Id: hal-02397878

<https://hal.science/hal-02397878>

Submitted on 6 Dec 2019

HAL is a multi-disciplinary open access archive for the deposit and dissemination of scientific research documents, whether they are published or not. The documents may come from teaching and research institutions in France or abroad, or from public or private research centers.

L'archive ouverte pluridisciplinaire **HAL**, est destinée au dépôt et à la diffusion de documents scientifiques de niveau recherche, publiés ou non, émanant des établissements d'enseignement et de recherche français ou étrangers, des laboratoires publics ou privés.

Short title: Electron transport pathways in chromoplasts

Title:

Electron transport pathways in isolated chromoplasts from *Narcissus pseudonarcissus* L.

Magda Grabsztunowicz¹, Paula Mulo¹, Frauke Baymann², Risa Mutoh^{3,#}, Genji Kurisu³,
Pierre Sétif⁴, Peter Beyer⁵, Anja Krieger-Liszkay^{4,*}

¹Molecular Plant Biology, University of Turku, 20520 Turku, Finland

²Bioénergétique et Ingénierie des Protéines, UMR 7281, CNRS - Aix-Marseille Université,
31, chemin Joseph Aiguier, 13409 Marseille, France

³Institute for Protein Research, Osaka University, Suita, Osaka, 565-0871, Japan

⁴Institute for Integrative Biology of the Cell (I2BC), CEA, CNRS, Univ Paris-Sud, Université
Paris-Saclay, 91198, Gif-sur-Yvette cedex, France

⁵Faculty of Biology, University of Freiburg, 79104 Freiburg, Germany

*Author for correspondence: Anja Krieger-Liszkay; e-mail anja.krieger-liszkay@cea.fr

A.K-L. conceived the project. M.G., P.M., A.K-L. designed and performed the experiments and analyzed the data. R.M., G. K. prepared Fd-Ga. A.K-L. wrote the article with contributions of P.S., P.B., P.M., M.G., F.B.

#Current address: Faculty of Science, Fukuoka University, Nanakuma, Jyonan-ku, Fukuoka, 814-0180, Japan

Abstract

During daffodil flower development, chloroplasts differentiate into photosynthetically inactive chromoplasts, which have lost functional photosynthetic reaction centers. Chromoplasts exhibit a respiratory activity reducing oxygen to water and generating ATP. Immunoblots revealed the presence of the plastid terminal oxidase (PTOX), the NAD(P)H dehydrogenase (NDH) complex, the cytochrome *b₆f* complex, ATP synthase and several isoforms of ferredoxin-NADP⁺ oxidoreductase (FNR) and of ferredoxin (Fd). Fluorescence spectroscopy allowed the detection of chlorophyll *a* in the cytochrome *b₆f* complex. Here we characterize the electron transport pathway of chromorespiration by using specific inhibitors for the NDH complex, the cytochrome *b₆f* complex, FNR and redox-inactive Fd in which the iron was replaced by gallium. Our data suggest an electron flow via two separate pathways, both reducing plastoquinone and using PTOX as oxidase. The first oxidizes NADPH via FNR, Fd, and cytochrome *b_h* of the cytochrome *b₆f* complex and does not result in the pumping of protons across the membrane. In the second, electron transport takes place via the NDH complex using preferentially NADH but also NADPH as electron donor. FNR and Fd are not involved in this pathway. The NDH-complex is responsible for the generation of the proton gradient. We propose a new model for chromorespiration which may also be relevant for the understanding of chlororespiration and for the characterization of the electron input from Fd to the cytochrome *b₆f* complex during cyclic electron transport in chloroplasts.

Introduction

Chromoplasts, the plastids of fruits and flowers, are essentially chlorophyll-free and characterized by the accumulation of carotenoids. In most cases, chromoplasts differentiate from chloroplasts or chloroplast-like precursors. The morphological changes taking place during the chloroplast-chromoplast transition have been investigated in detail in case of the daffodil flower (*Narcissus pseudonarcissus*) (Liedvogel et al., 1976). The dismantling of the thylakoid membranes and the *de-novo* formation of a complex concentrically stacked membrane system represent highly energy demanding processes involving several anabolic pathways like massive carotenoid and lipid synthesis (Kleinig and Liedvogel, 1980; Angaman et al., 2012). In the absence of photosynthesis, the required energy is thought to be imported from the cytoplasm or mitochondria into the stroma in the form of ATP and NADPH by the phosphate and malate/dicarboxylate translocators (Renné et al., 2003; Flügge et al., 2011; Bailleul et al., 2015). However, contributing to the energy balance of the system, chromoplasts exhibit a respiratory activity associated with their membrane system. The chromoplast respiratory chain uses NADH or NADPH as electron donor, involves plastoquinone and generates a proton motive force which is used to synthesize ATP (Mayer et al., 1990; Nievelstein et al., 1995; Morstadt et al., 2002; Pateraki et al., 2013). Chromoplasts from different species use either NADPH or NADH as the preferred electron donor. Addition of NADH resulted in higher respiratory activity in tomato chromoplasts than NADPH (Renato et al., 2014) while the opposite was found with daffodil chromoplasts (Nievelstein et al., 1995). Chromorespiration may be related to a similar process in chloroplasts, chlororespiration, first been described by Bennoun (1982) as a light-independent electron transport pathway from NAD(P)H to O₂

The tomato chromoplast proteome revealed the presence of NDH complex subunits and of the cytochrome *b₆f* complex (Barsan et al., 2012; Wang et al., 2013) rendering these two likely components of the respiratory electron transport chain. Furthermore, it has been suggested that a type II NDH contributes to the reduction of the PQ pool (Renato et al., 2014). The participation of the cyt *b₆f* complex in chromorespiration is corroborated by the partial sensitivity of ATP synthesis to DBMIB, an inhibitor of the cyt *b₆f* complex (Renato et al., 2014). In contrary to chloroplast electron transport reactions, cytochrome *c₆* instead of plastocyanin was proposed to act as electron acceptor of the high potential chain of the cyt *b₆f* complex to donate electrons to a putative cyt *c₆* oxidase which would act as terminal oxidase (Renato et al., 2014; 2015). However in plastids, there is no evidence for the presence of a

classical mitochondrial-type cyt *c* oxidase and evidence for a high potential electron transport chain is lacking. In tomato chromoplasts, the respiratory activity depends to a large extent on the plastid terminal oxidase PTOX (Renato et al., 2014). PTOX is not only involved in the respiratory activity of these organelles but is also required for carotenoid biosynthesis in photosynthetically inactive chromoplasts. It regenerates the cofactor of the phytoene and ζ -carotene desaturases, plastoquinone, which is reduced upon carotene desaturation (Carol et al., 1999; Gemmecker et al., 2015; Brausemann et al., 2017).

Open questions pertain to the composition of the chromorespiratory electron transport chain and the pathway of electron flux. The implication of the cyt *b₆f* complex remains obscure in the absence of evidence for a high potential electron transport chain involving the Rieske protein. In addition, the question arises on the pigment bound to the cyt *b₆f* complex. Chromoplasts seem to be completely devoid of chlorophyll (Liedvogel et al., 1976) while chlorophyll *a* is a constituent of the chloroplast *b₆f* complex in chloroplasts that is replaced by protochlorophyll in etioplasts (Reisinger et al., 2008). This indicates that either chlorophyll itself or a chlorophyll derivative is required to attain structural integrity and functionality of the cyt *b₆f* complex. Clarification is also needed on the nature of the NAD(P)H electron acceptor. In chloroplasts, electrons enter the chlororespiratory chain through reduced ferredoxin (Fd_{red}) to subsequently be delivered to cyt *b₆f* and the NDH complex (Yamamoto et al., 2011; Peltier et al., 2016).

We used daffodil chromoplasts to further characterize the chromorespiratory pathway and to investigate the roles of the cyt *b₆f* and NDH complexes in establishing the proton motive force. We also scrutinized the role of Fd in chromorespiration by replacing it with a redox-inactive version in which Fe of the FeS cluster is replaced by Ga (Mutoh et al., 2015). Furthermore, we used absorption and fluorescence spectroscopy to characterize the properties of the chromoplast cyt *b₆f* complex. Based on the differential effects of a variety of inhibitors we propose a model in which two separate electron transport pathways coexist. Of these, one is non-proton-pumping. It involves NADPH and ferredoxin-NADP⁺ oxidoreductase (FNR)/ferredoxin (Fd) and the cyt *b₆f* complex while the other represents an NAD(P)H-dependent proton-pumping pathway that employs the NDH complex, but is independent of FNR/Fd.

Results

Two distinct redox pathways involved in chromorespiration?

'Grade A' chromoplasts isolated from the inner corollae of fully opened daffodil flowers show an NADPH-dependent respiratory activity that is linked to an alkalization of the medium documenting the pumping of protons. These activities depend on PTOX since both are sensitive to octylgallate (OG), a known PTOX inhibitor (Josse et al., 2003; Fig. 1). The H^+/O_2 ratio is slightly below 1 corresponding to a $H^+/2e^-$ ratio of slightly below 2 (Fig. 1; Table 1), showing that the generated proton gradient is small compared to values obtained in photosynthetic or respiratory electron transport with typical ratios of 10 $H^+/2e^-$ in respiration. Addition of the uncoupler nigericin stopped the alkalization of the medium, as expected, but had no effect on the respiratory activity. The low H^+/O_2 ratio found for daffodil chromoplasts led us to suspect the presence of two distinct electron transport pathways involved in the overall respiratory activity, one leading to the formation of a transmembrane proton gradient required for ATP synthesis while the other representing a futile pathway using reduction equivalents to generate heat.

Possible redox-active constituents of chromorespiration

Immunoblots were carried out to identify proteins that may be involved in chromorespiration. As shown in Fig. 2, the NDH complex subunit H (NDH-H), PTOX, the ATP-synthase β -subunit, ferredoxin (Fd), the cyt *b₆f* complex subunit cyt *f*, the Fd-plastoquinone reductase in photosynthetic cyclic electron flow PGRL1 (Hertle et al., 2013) and the ferredoxin-NADP⁺ oxidoreductase (FNR) were all well detected in mature chromoplasts. Additional immunoblots served for differentiating between FNR and Fd isoforms (Fig. 3). Arabidopsis contains two functionally redundant leaf-type FNR isoforms (L-FNR1 and L-FNR2; Lintala et al., 2007; 2009) and two distinct leaf-type Fd isoforms (AtFd1 and AtFd2) (Green et al., 1991; Hanke et al., 2004, 2005; Hanke and Mulo, 2013). In addition, two root-type FNRs (R-FNR1 and R-FNR2) and a root-type Fd (AtFd3) are enriched in root plastids (Morigasaki et al., 1993; Hanke et al., 2004). R-FNRs accept electrons from NADPH to reduce root-type Fd, the latter providing reducing power to a number of activities, such as fatty acid biosynthesis and redox regulation (Hanke and Mulo, 2013). Intriguingly, the leaf- and root-type specific FNR and Fd antibodies used recognized several protein bands (Fig. 3) indicating that chromoplasts contain at least three distinct FNR and two to three Fd

isoforms, most probably representing leaf- and root-type isoforms. The two L-FNR isoforms were distributed between the soluble (S) and membrane (M) chromoplast subfractions (Fig. 3a) similar to the situation found in chloroplasts (Hanke et al., 2005; Lintala et al., 2007). In contrast, R-FNR appeared as soluble protein only (Fig. 3a). Moreover, Blue Native gel electrophoresis followed by immunoblotting revealed that FNR existed in several large protein complexes in chromoplasts, resembling the pattern reported for thylakoid membranes (Fig. 3b; Benz et al., 2009). Chromoplast membranes also contained the TROL protein, which is known in chloroplasts to exist in a thylakoid protein complex together with L-FNR (Fig. 3c; Juric et al., 2009).

The FNR-, Fd- and cyt *b₆f*-dependent branch of chromorespiration

To show the participation of Fd in the chromorespiratory pathway, a redox-inactive Fd from *Thermosynechoccus elongatus* in which the FeS cluster iron is replaced by gallium (Fd-Ga; Mutoh et al., 2015) was added to the chromoplasts. Redox-inactive Fd has recently been used to study Fd binding to photosystem I blocking Fd reduction (Mignéé et al., 2017). It can be used as a general tool for the study of Fd-dependent electron transport reactions. As shown in Fig. 4, the addition of Fd-Ga inhibited O₂ consumption up to 80% with a K_i ≈ 100 nM. Addition of an excess of *T. elongatus* Fd-Fe to the Fd-Ga-inhibited samples restored the original activity. When DBMIB, an inhibitor of the cyt *b₆f* complex (see below), was added in addition to Fd-Ga, no further inhibition was observed. These data show that the main respiratory pathway in chromoplasts involves Fd as the electron donor. Diphenylene iodonium (DPI) inhibited the diaphorase activity of FNR, isolated from *Synechocystis* PCC6803 (Suppl. Fig. 1), as expected for an inhibitor of flavoproteins (O'Donnell et al., 1993). Its inhibitory effect on the O₂-consumption by chromoplasts (Table 1b) demonstrates that FNR acts as a Fd-reducing partner in the Fd-dependent chromorespiratory pathway. However, when NADPH was replaced by NADH, DPI had almost no inhibitory effect in chromoplasts (Table 1b), in accordance with the high specificity of FNR for NADPH (Morigasaki et al., 1990; Medina et al., 2001).

To determine whether Fd donates electrons to the cyt *b₆f* complex, the effects of its specific inhibitors DBMIB and DNP-INT and the effects of the ferredoxin-quinone reductase (FQR)-inhibitor antimycin A were studied. As shown in Fig. 5, the main respiratory pathway takes in fact this route since all inhibitors tested inhibit O₂ consumption to 70-80 % of (Fig.

5). DBMIB is the most effective, inhibiting up to 80 % of the O₂ consumption with K_i ≈ 2 μM. DNP-INT, an inhibitor of the Cyt *b₆f* complex with binding properties different to DBMIB (Trebst et al., 1979), inhibited about 70 % with a K_i ≈ 25 μM. Addition of Fd-Ga did not lead to a further inhibition of the O₂ consumption as shown in Fig. 5A for DBMIB (Fig. 5a, cross symbol). The same effect was found when respiration was inhibited with Fd-Ga followed by the addition of DBMIB (Fig. 4, cross symbol). Antimycin A, which inhibits cyclic electron flow in chloroplasts depending on the FQR (Bendal and Manasse, 1995; Munekage et al., 2002; Hertle et al., 2013), inhibits chromorespiration to about 60 % with a K_i ≈ 25 μM, indicating that PGRL1/PGR5 are involved in the electron transport reaction although we could only detect PGRL1 in the immunoblots (Fig. 2). All inhibitors tested have in common that none is capable in completely abolishing the respiratory activity. This indicates that the remaining activity is neither Fd-dependent nor does it involve the cyt *b₆f* complex.

The NDH complex-dependent branch of chromorespiration

To further distinguish between the two electron transport pathways, NADH was used as electron donor, in addition to NADPH (Table 1b). The respiratory activity was 25% lower when 200 μM NADH instead of 200 μM NADPH was used. The NADH-dependent pathway was not sensitive to DBMIB, only marginally sensitive to DPI but it was strongly inhibited by Cibacron Blue 3G-A and completely blocked by rotenone (Table 1b). Cibacron Blue 3G-A mimics adenine nucleotides like NADH and binds to the nucleotide-binding sites of several enzymes (Prester et al., 1992). Rotenone is a well-known inhibitor of the complex I of mitochondria, and it inhibits NADPH-oxidation by the NDH complex competitively (Hu et al., 2013). The inhibitory effect of rotenone and Cibacron Blue 3G-A on the NADH-dependent pathway shows that the electron transport proceeds via the NDH complex. Most importantly, rotenone inhibition was also accompanied by the complete absence of medium alkalization (Table 1a) documenting that this branch is responsible for proton translocation. This pathway is thus proton pumping; it utilizes the NDH complex but does not employ neither the cyt *b₆f* complex nor Fd. None of the two electron transport pathways was affected by KCN (Table 1b) documenting the absence of mitochondrial contaminations in the chromoplast preparations used.

Functionality of the cyt *b₆f* complex in chromoplasts

A spectrum composed of cyt *f* and cyt *b* characteristics (Fig. 6) was obtained when the spectrum of the chromoplast membrane preparation was subtracted from the one obtained in the presence of ferricyanide. Cyt *f* shows a minimum at 554 nm, cyt *b_l* and cyt *b_h* at 564 nm (Alric et al., 2005). This shows that the cytochromes of the chromoplast membranes were in the reduced state in the preparations used. The buffer in which the chromoplast preparations were stored contained 1 mM 1,4-dithioerythritol (midpoint redox potential of -0.33V) which explains this fact. No further changes were observed when dithionite was added to the sample. Cyt *b_h* appears to be partially reduced and dithionite may have no easy access to it.

The problem with the functionality of the cyt *b_{6f}* complex resides in the fact that chlorophyll *a* or protochlorophyll is needed (see Introduction) while chromoplast membranes did not show any absorbance characteristic for chlorophyll, even at very high sample concentrations. The spectra were dominated by carotenoid absorption. However, when fluorescence was measured, an emission was observed with a maximum at 684 nm (Fig. 7), identical to the one observed with the isolated cyt *b_{6f}* complex from the green alga *B. cortulans* (Zuo et al., 2006). In *Synechocystis* 6803 (Peterman et al., 1998) and in *Chlamydomonas reinhardtii* (Pierre et al., 1997), the fluorescence maximum of the isolated complex was found at about 10 nm shorter wavelength. Upon acetone extraction of chromoplasts, the fluorescence spectrum shifted by 16 nm toward shorter wavelength with a maximum of 668 nm that is characteristic for chlorophyll *a* (Fig. 7, solid line). According to these data, the chromoplast cyt *b_{6f}* complex contains chlorophyll *a*, like in chloroplasts. The amount of chl *a* per cyt *b_{6f}* was estimated by using a calibration curve obtained by measuring the fluorescence of known amounts of pure chlorophyll *a* (Fig. 7, inset). By comparing the obtained value for chl *a* and the cyt *b* absorption shown in Fig. 6, using the extinction coefficient of cyt *b* given in Alric et al (2005), an approximate 1:1 stoichiometry is obtained, as expected.

Discussion

The chromorespiratory pathway as a whole involves the plastid terminal oxidase PTOX, as witnessed by the pronounced inhibition effect of octylgallate on both, oxygen consumption and alkalization (Fig 1, Table 1). However, apart from this common constituent, we provide evidence for the presence of two co-existing sub-branches with only one capable in pumping protons. In daffodil chromoplasts, NADPH-dependent O₂-consumption proceeds

via both branches while NADH serves as substrate for only one. This selectivity for reduction equivalents is one clear-cut distinction that can be made. It is reflected in the different molecular constituents involved.

A pathway that does not pump protons

FNR, Fd, the cyt *b₆f* and finally quinones and PTOX are central to this pathway that shows high selectivity for NADPH (Table 1). The involvement of these complexes is inferred by the strong effect of the FNR inhibitor DPI, Fd-Ga and cyt *b₆f* inhibitors (Figs. 4, 5). The presence of a fully functional *b₆f* complex in chromoplasts is supported by detection of cyt *b* and *f* in redox-induced optical difference spectra and by the presence of chlorophyll *a*. Constituents of this pathway were also well detectable by immunoblots in these fully developed chromoplasts (Figs 2, 3).

In daffodil chromoplasts, several FNR and Fd isoforms were detected (Fig. 3), raising questions on their specificity to donate electrons from NADPH to the non-proton pumping branch of the electron transport chain. From a thermodynamic and structural perspective (Shinohara et al., 2017), the root FNR:Fd complex favors the electron transfer from NADPH to Fd while the leaf FNR:Fd complex facilitates the reverse. It is conceivable that the two detected FNR types (Fig. 3a) may both function in NADPH oxidation, but there is currently no knowledge on specific interactions with ferredoxin isoforms, on the roles of membrane-bound and soluble FNRs and on the composition of the FNR-containing protein complexes that may exhibit modulated specificity or activity.

By activity, this branch represents the dominating one. In the presence of inhibitors of the cyt *b₆f* complex, respiration was affected by 70-80% (Fig. 5, Table 1). However, the alkalization of the medium remained almost unaffected (Table 1). This non-proton pumping part of the chromorespiratory pathway via the cyt *b₆f* complex may generate the heat needed to dissipate volatile terpenoids synthesized by flower chromoplasts (Mettal et al., 1988) serving as pollinator attractants. A similar function has been attributed to the electron transport in mitochondria involving the alternative oxidase AOX for example in *Arum maculatum* (Wagner et al., 2008).

A pathway that pumps protons

We assign the remaining 20-30% respiration found in the presence of cyt *b₆f* complex inhibitors to a second branch that depends on the NDH complex. We show that this remaining activity can use NADH as an electron donor. This assignment is based on the inhibitory effect of Cibacron Blue 3G-A and rotenone on the ca. 20 % respiratory activity obtained with NADPH. Rotenone, a well-known inhibitor of the mitochondrial complex I, has been shown to also inhibit isolated NDH complex from *Thermosynechococcus elongatus* (Hu et al., 2013). This branch is affected by neither the FNR-inhibitor DPI, Fd-Ga, nor DBMIB and DNP-INT. This confirmed that this branch is independent of FNR/Fd/cyt *b₆f*.

This observation contradicts at first glance the data reported on NDH-dependent electron transport in thylakoid membranes where Fd has been identified as electron donor to the NDH complex (Yamamoto et al., 2011). In this study, NDH activity was measured using chlorophyll fluorescence by following the post illumination fluorescence rise in freshly ruptured chloroplasts. External Fd had to be added to obtain the fluorescence rise. Fd-Ga should be able to compete with Fd-Fe in chromoplasts if the observed respiration was dependent on electron donation from Fd_{red} to the NDH complex, comparable to the situation in chloroplasts. This was clearly not the case. The protein composition of the chromoplast NDH complex may differ from that of the chloroplast and an NAD(P)H-oxidizing module different from FNR:Fd seems to be present in the daffodil chromoplasts, a module which would be absent in the chloroplast enzyme. This is in line with data reporting differences in the protein composition and enzymatic activity between NDH complexes from etioplasts and chloroplasts with a comparatively higher NADH dehydrogenase activity found with the former (Guéra et al., 2000).

According to our data, this pathway branch pumps protons yielding the proton gradient to drive ATP synthesis via the H⁺-ATP synthase complex, as previously been demonstrated with daffodil chromoplasts (Morstadt et al., 2002). This pathway is mainly based on the observation that rotenone, inhibiting specifically this branch (while leaving the other one unaffected) concomitantly inhibits the alkalization of the medium. In an analogy to the mitochondrial complex I, this branch would be expected to pump 4 protons per NADH oxidized.

The model and remaining questions

We propose that chromorespiration utilizes two different pathways. The proton-pumping branch consists of the NDH complex transferring electrons from NADH to quinone and implies the efficient proton-pumping activity of this complex (Strand et al., 2017). The non-proton pumping branch relies on electron transfer from NADPH to Fd catalyzed by FNR (Fig. 8) and further electron transfer from Fd_{red} via the cyt *b₆f* complex to plastoquinone. Both pathways are interlinked at the stage of plastoquinol oxidation by PTOX as evidenced by their sensitivity to octy gallate.

The main question related to the model presented here pertains to the function of the cyt *b₆f* complex in the non-proton pumping branch. Cytochrome *b₆f* complexes are known to participate on the build-up of the proton motive force when electrons travel according to the Q-cycle model through the complex. We propose that only the stroma-facing side of the cyt *b₆f* complex including the Q_i site, cyt *b_h* and potentially cyt *c_i* and/or PGR5/PGRL1 is operating (Fig. 9). Electrons from NADPH would reach the Q_i-site quinone via heme *c_i* and *b_h* and after two turnovers a quinol could leave the site to become oxidized by PTOX. In chromoplasts, an active high potential chain via cyt *f* and plastocyanin does not exist since there is no photosystem I. Unlike in tomato chromoplasts (Renato et al., 2014), KCN did not inhibit the electron transport in daffodil chromoplasts (Table 1) and therefore, a participation of the mitochondrial cytochrome *c* oxidase as putative partner of a high potential chain can be excluded. According to our model (Fig. 9), PQ at the Q_o site and Cyt *b_l* do not participate in the chromorespiratory electron transport, no Q-cycle takes place and consequently, no protons are translocated. In chromoplasts significantly higher concentrations of DBMIB and DNP-INT than in chloroplasts are necessary to inhibit the electron transport activity. Here we determined a K_I of 2 μM for DBMIB, which is significantly higher than the values reported for Q_o site inhibition in chloroplasts (K_I=10-20 nM, depending on the chlorophyll concentration; Graan and Ort, 1986). In chloroplasts, high concentrations of DBMIB (≥10 μM) inhibit the PQ reduction at the Q_i site while low concentrations (complete inhibition at 1 μM DBMIB) inhibit specifically PQH₂ oxidation at the Q_o-site (Trebst et al., 1978; Barbagallo et al., 1999). The binding site of DNP-INT is less clear. Trebst and coworkers (1978) reported binding at the same site like DBMIB at high concentrations. Barbagallo et al. (1999) reported binding to the Q_o-site. The action of these inhibitors in chromoplasts led us to propose that they inhibit PQ reduction at the Q_i site. Electron donation from Fd_{red} to plastoquinone via heme *c_i* may also act as electron input module in cyclic electron flow in chloroplasts.

The second question concerns the implication of PGR5/PGRL1 in chromorespiration. Antimycin A, which inhibits the FQR-dependent cyclic electron flow in chloroplasts, inhibits chromorespiration, indicating the involvement of PGRL1/PGR5 in addition to the cytochrome *b₆f* complex. It has been proposed by Hertle and coworkers (Hertle et al., 2013) that PGRL1 can reduce PQ without involvement of the cyt *b₆f* complex. Since the chromorespiratory activity was inhibited by several known cyt *b₆f* inhibitors, we discard the option that PGRL1 reduces PQ directly. However, we do not exclude PGRL1 participation, potentially forming together with PGR5 the electron input module of cyt *b₆f*, allowing Fd_{red} to donate electrons to cyt *b_h*.

Discussion of previous chromorespiratory pathways models

Our model does not support previously published suggestions for respiratory pathways of non-green plastids in several ways. The participation of the cyt *b₆f* complex in chromorespiration or etiorespiration has previously been implied (Pateraki et al., 2013; Renato et al., 2014; Kambakam et al., 2016). However, the previously suggested proton pumping activity of the cyt *b₆f* complex required for ATP synthesis is not supported by our data that greatly favor the NDH complex for this purpose. This is in line with findings on the highly efficient proton pumping activity of the NDH complex in chloroplasts (Strand et al., 2017).

Renato and coworkers (2014; 2015) have also suggested a branched electron transport in tomato chromoplasts. However, they proposed one branch accepting electrons from NADH through NDH and the other branch accepting electrons from NADPH through a type II NADPH dehydrogenase delivering electrons to cyt *b₆f*. This is contrast to our data showing that NADPH is mainly oxidized by FNR/Fd/cyt *b₆f*. Similar to our data (Table 1b), these authors reported on a strong inhibition of the NADPH-dependent electron transport by DPI and a weak inhibition of the NADH-dependent electron transport. They assigned the former to an electron transport pathway involving the NDH complex. However, our data assign DPI sensitivity to the FNR/Fd/cyt *b₆f*-dependent electron transport while the NDH-dependent branch is DPI-insensitive (Table 1b). The inefficiency of DPI on the mitochondrial complex I (Lambert et al. 2008) is in agreement with our observation.

In etioplasts, Fd_{red} has been suggested as substrate for the NDH complex (Kambakam et al., 2016), an electron transport pathway which can be ruled out for daffodil chromoplasts since

Fd-Ga did not inhibit the NDH-dependent pathway. However, we cannot exclude that etiorespiration as well as chlororespiration might in fact use Fd_{red} as electron donor for the NDH complex. The effect of Fd-Ga on these pathways has not yet been investigated.

Concluding remarks

In daffodil chromoplasts, chromorespiration takes place via a proton-pumping pathway employing the NDH complex using NAD(P)H as substrate and a non-proton-pumping pathway depending on NADPH/FNR/Fd/Cyt *b₆f* complex. These two electron input modules may function in a similar way in chloroplasts in the dark (chlororespiration). Chromoplasts are well suited to study these types of respiratory pathways since their membranes lack functional photosystems, thus removing a substantial portion of the electron transfer complexity present in chloroplasts. This experimental system may serve to answer the question of the importance of the contribution of cyclic electron flow via the cyt *b₆f* complex in chloroplasts to the proton motif force. Furthermore, Fd-Ga may serve as a unique tool to study the role of Fd in cyclic electron flow via both, the NDH complex and the cyt *b₆f* complex, in chloroplasts.

Materials and Methods

Chromoplast preparation

Chromoplasts of the inner coroneae of fully opened flowers of daffodil (*Narcissus pseudonarcissus* L. cv Dutch Master), developmental stage IV (Al-Babili et al. 1996), were isolated according to the method of Liedvogel et al. (1976) using a step gradient in which chromoplasts accumulate at the 15%/30% ('grade A') and 30%/40% ('grade B') sucrose interphases. The isolated chromoplasts were suspended in 100 mM Tris/HCl pH 7.4, 10 mM MgCl₂, 1 mM 1,4-dithioerythritol. The preparations were stored at -80°C. The protein content of the chromoplast preparation was determined using amido black. For all experiments only 'grade A' chromoplast preparations were used. For subfractionation, chromoplasts were lysed with shock buffer (10 mM HEPES-KOH, pH 7.6, 5 mM Sucrose, 5 mM MgCl₂), and soluble and membrane fractions were separated by centrifugation, as described by Grabsztunowicz et al. (2015).

Protein extraction

Total proteins of leaf and root material were extracted from hydroponically grown *Narcissus* plants as described by Lehtimäki et al. (2014) and Raorane et al. (2016), respectively.

Chromorespiration

The respiratory activity of chromoplasts was measured with a Liquid-Phase Oxygen Electrode Chamber (Hansatech Instruments, Norfolk, UK) at 20°C. For simultaneous measurements of O₂-consumption and pH, a pH-electrode was inserted on the top of the O₂-electrode chamber. Chromoplasts were resuspended in a low strength buffer (0.1 mM Tris/HCl pH 7.4, 10 mM MgCl₂) to allow measuring alkalization of the medium.

SDS-PAGE, Blue Native-PAGE and Western Blotting

Chromoplast proteins were separated using SDS-PAGE (8% or 12% acrylamide, as indicated) and the gels were blotted onto a nitrocellulose (Anti-PTOX; Anti-ATPase; anti-FNR; anti-NDH-H; anti-Fd; anti-PGRL1 and anti-PGR5) or a PVDF membrane (anti-TROL; anti AtFd1; anti AtFd3; anti-L-FNR; anti-R-FNR), blocked with 5% milk, and proteins immunodetected using the ECL system (GE Healthcare). For separation of protein complexes, BN-PAGE was performed as given in Sirpiö et al. (2007). BN gels were electro-blotted onto the PVDF membrane and used for immunodetection. The following polyclonal antibodies were used: Anti-PTOX (provided by M. Kuntz, CEA Grenoble), anti-ATPase (β -subunit of ATP synthase; Agrisera, Vännäs, Sweden), anti-FNR (ferredoxin-NADP reductase, provided by W. Oettmeier, Ruhr Universität Bochum, Germany), leaf-type and root-type FNR antibodies (provided by P.E. Jensen, University of Copenhagen, Denmark and T. Hase, Osaka University, Japan, respectively), anti-NDH-H (provided by D. Rumeau, CEA Cadarache, France), anti-Fd (provided by B. Lagoutte, CEA Saclay, France; AtFd3 provided by G. Hanke, Queen Mary University of London, UK; AtFd1 Agrisera, Vännäs, Sweden), anti-PGRL1 and anti-PGR5 (provided by T. Shikanai, University of Kyoto, Japan) and anti-TROL (provided by G. Hanke, Queen Mary University of London, UK).

Absorption and fluorescence spectra

UV-vis absorption changes were measured with a high sensitivity in-house built spectrophotometer (Joliot et al., 1980). Fluorescence was monitored with a CARY Eclipse spectrophotometer (Varian, Agilent, Santa Clara, CA, USA). Samples were excited at 435 nm, and the emission was recorded from 650 to 800 nm. Chromoplasts (40 $\mu\text{g ml}^{-1}$ protein) were suspended in either 100 mM Tris/HCl pH 7.4, 10 mM MgCl_2 or in 100% acetone. The acetone suspension was vortexed for pigment extraction, centrifuged at 12000 x g for 3 min and the supernatant was collected. The chl *a* content was determined with the aid of a calibration curve made with chl *a* solutions in acetone ($\epsilon=78.78 \times 10^3 \text{ l mol}^{-1} \text{ cm}^{-1}$ in 100% acetone). Isolated Chl *a* was provided by H. Paulsen, University of Mainz, Germany.

Acknowledgements

We thank Jean Alric, CEA Cadarache, for his help with measuring the cytochrome absorption spectra and for providing the model spectra. Ms. Anniina Lepistö is thanked for skillful technical assistance. This study was financially supported by the Academy of Finland (307335 ‘Centre of Excellence in Molecular Biology of Primary Producers’ for PM and MG).

References

- Al-Babili S, von Lintig J, Haubruck H, Beyer P** (1996) A novel, soluble form of phytoene desaturase from *Narcissus pseudonarcissus* chromoplasts is Hsp70-complexed and competent for flavinylation, membrane association and enzymatic activation. *Plant Journal* **9**: 601-612
- Alric J, Pierre Y, Picot D, Lavergne J, Rappaport F** (2005) Spectral and redox characterization of the heme c(i) of the cytochrome b(6)f complex. *Proc Natl Acad Sci U S A* **102**: 15860-15865
- Angaman MD, Petrizzo R, Hernandez-Gras F, Romero-Segura C, Pateraki I, Busquets M, Boronat A** (2012) Precursor uptake assays and metabolic analyses in isolated tomato fruit chromoplasts. *Plant Methods* **8**:
- Bailleul B, Berne N, Murik O, Petroustos D, Prihoda J, Tanaka A, Villanova V, Bligny R, Flori S, Falconet D, Krieger-Liszkay A, Santabarbara S, Rappaport F, Joliot P, Tirichine L, Falkowski PG, Cardol P, Bowler C, Finazzi G** (2015) Energetic coupling between plastids and mitochondria drives CO₂ assimilation in diatoms. *Nature* **524**: 366-369

- Barbagallo RP, Finazzi G, Forti G** (1999) Effects of inhibitors on the activity of the cytochrome b(6)f complex: Evidence for the existence of two binding pockets in the luminal site. *Biochemistry* **38**: 12814-12821
- Barsan C, Zouine M, Maza E, Bian W, Egea I, Rossignol M, Bouyssie D, Pichereaux C, Purgatto E, Bouzayen M, Latche A, Pech JC** (2012) Proteomic Analysis of Chloroplast-to-Chromoplast Transition in Tomato Reveals Metabolic Shifts Coupled with Disrupted Thylakoid Biogenesis Machinery and Elevated Energy-Production Components. *Plant Physiology* **160**: 708-725
- Bendall DS, Manasse RS** (1995) Cyclic photophosphorylation and electron transport. *Biochim Biophys Acta* **1229**: 23-38
- Bennoun P** (1982) Evidence for a respiratory chain in the chloroplast. *Proc Natl Acad Sci U S A* **79**: 4352-4356
- Benz JP, Stengel A, Lintala M, Lee YH, Weber A, Philippar K, Gügel IL, Kaieda S, Ikegami T, Mulo P, Soll J, Böltner B** (2009) Arabidopsis Tic62 and ferredoxin-NADP(H) oxidoreductase form light-regulated complexes that are integrated into the chloroplast redox poise. *Plant Cell* **21**: 3965–3983
- Brausemann A, Gemmecker S, Koschmieder J, Ghisla S, Beyer P, Einsle O** (2017) Structure of Phytoene Desaturase Provides Insights into Herbicide Binding and Reaction Mechanisms Involved in Carotene Desaturation. *Structure* **25**: 1222-1232
- Carol P, Stevenson D, Bisanz C, Breitenbach J, Sandmann G, Mache R, Coupland G, Kuntz M** (1999) Mutations in the Arabidopsis gene *immutans* cause a variegated phenotype by inactivating a chloroplast terminal oxidase associated with phytoene desaturation. *Plant Cell* **11**: 57-68
- Flügge UI, Häusler RE, Ludewig F, Gierth** (2011) The role of transporters in supplying energy to plant plastids. *J Exp Bot.* **62**: 2381-2392
- Gemmecker S, Schaub P, Koschmieder J, Brausemann A, Drepper F, Rodriguez-Franco M, Ghisla S, Warscheid B, Einsle O, Beyer P** (2015) Phytoene Desaturase from *Oryza sativa*: Oligomeric Assembly, Membrane Association and Preliminary 3D-Analysis. *Plos One* **10**: e0131717
- Graan T, Ort DR** (1986) Quantitation of 2,5-Dibromo-3-Methyl-6-Isopropyl-Para-Benzoquinone Binding-Sites in Chloroplast Membranes - Evidence for A Functional Dimer of the Cytochrome-B6F Complex. *Archives of Biochemistry and Biophysics* **248**: 445-451
- Grabsztunowicz M, Gorski Z, Lucinski R, Jackowski G** (2015) A reversible decrease in ribulose 1,5-bisphosphate carboxylase/oxygenase carboxylation activity caused by the aggregation of the enzyme's large subunit is triggered in response to the exposure of moderate irradiance-grown plants to low irradiance. *Physiologia Plantarum* **154**: 591-608
- Green LS, Yee BC, Buchanan BB, Kamide K, Sanada Y, Wada K** (1991) Ferredoxin and ferredoxin-NADP reductase from photosynthetic and nonphotosynthetic tissues of tomato. *Plant Physiology* **96**: 1207–1213

- Guera A, de Nova PG, Sabater B** (2000) Identification of the Ndh (NAD(P)H-plastoquinone-oxidoreductase) complex in etioplast membranes of barley: Changes during photomorphogenesis of chloroplasts. *Plant and Cell Physiology* **41**: 49-59
- Hanke GT, Kimata-Arigo Y, Taniguchi I, Hase T** (2004) A post genomic characterization of Arabidopsis ferredoxins. *Plant Physiology* **134**: 255-64
- Hanke G, Mulo P** (2013) Plant type ferredoxins and ferredoxin-dependent metabolism. *Plant Cell & Environment* **36**: 1071–1084
- Hanke GT, Okutani S, Satomi Y, Takao T, Suzuki A, Hase T** (2005) Multiple iso-proteins of FNR in Arabidopsis: evidence for different contributions to chloroplast function and nitrogen assimilation. *Plant Cell Envir* **28**: 1146-1157
- Hertle AP, Blunder T, Wunder T, Pesaresi P, Pribil M, Armbruster U, Leister D** (2013) PGRL1 Is the elusive ferredoxin-plastoquinone reductase in photosynthetic cyclic electron flow. *Mol Cell* **49**: 511-523
- Hu P, Lv J, Fu PC, Mi HL** (2013) Enzymatic characterization of an active NDH complex from *Thermosynechococcus elongatus*. *Febs Letters* **587**: 2340-2345
- Joliot P, Beal D, Frilley B** (1980) A New Spectrophotometric Method for the Study of Photosynthetic Reactions. *Journal de Chimie Physique et de Physico-Chimie Biologique* **77**: 209-216
- Josse EM, Alcaraz JP, Laboure AM, Kuntz M** (2003) In vitro characterization of a plastid terminal oxidase (PTOX). *European Journal of Biochemistry* **270**: 3787-3794
- Jurić S, Hazler-Pilepić K, Tomasić A, Lepedus H, Jelčić B, Puthiyaveetil S, Bionda T, Vojta L, Allen JF, Schleiff E, Fulgosi H** (2009) Tethering of ferredoxin:NADP⁺ oxidoreductase to thylakoid membranes is mediated by novel chloroplast protein TROL. *Plant J* **60**: 783–794
- Kambakam S, Bhattacharjee U, Petrich J, Rodermel S** (2016) PTOX Mediates Novel Pathways of Electron Transport in Etioplasts of Arabidopsis. *Molecular Plant* **9**: 1240-1259
- Kleinig H, Liedvogel B** (1980) Fatty-Acid Synthesis by Isolated Chromoplasts from the Daffodil - Energy-Sources and Distribution Patterns of the Acids. *Planta* **150**: 166-169
- Lambert AJ, Buckingham JA, Boysen HM, Brand MD** (2008) Diphenyleneiodonium acutely inhibits reactive oxygen species production by mitochondrial complex I during reverse, but not forward electron transport. *Biochimica et Biophysica Acta-Bioenergetics* **1777**: 397-403
- Lehtimäki N, Koskela MM, Dahlström KM, Pakula E, Lintala M, Scholz M, Hippler M, Hanke GT, Rokka A, Battchikova N, Salminen TA, Mulo P** (2014) Posttranslational Modifications of FERREDOXIN-NADP(+) OXIDOREDUCTASE in Arabidopsis Chloroplasts. *Plant Physiology* **166**: 1764-1776
- Liedvogel B, Sitte P, Falk H** (1976) Chromoplasts in Daffodil - Fine-Structure and Chemistry. *Cytobiologie* **12**: 155-174

- Lintala M, Allahverdiyeva Y, Kidron H, Piippo M, Battchikova N, Suorsa M, Rintamäki E, Salminen TA, Aro EM, Mulo P** (2007) Structural and functional characterization of ferredoxin-NADP⁺-oxidoreductase using knock-out mutants of *Arabidopsis*. *Plant J* **49**: 1041-1052
- Lintala M, Allahverdiyeva Y, Kangasjärvi S, Lehtimäki N, Keränen M, Rintamäki E, Aro EM, Mulo P** (2009) Comparative analysis of leaf-type ferredoxin-NADP oxidoreductase isoforms in *Arabidopsis thaliana*. *Plant J* **57**: 1103–1115
- Mayer MP, Beyer P, Kleinig H** (1990) Quinone Compounds Are Able to Replace Molecular-Oxygen As Terminal Electron-Acceptor in Phytoene Desaturation in Chromoplasts of Narcissus-Pseudonarcissus L. *European Journal of Biochemistry* **191**: 359-363
- Medina M, Luquita A, Tejero J, Hermoso J, Mayoral T, Sanz-Aparicio J, Grever K, Gomez-Moreno C** (2001) Probing the determinants of coenzyme specificity in ferredoxin-NADP(+) reductase by site-directed mutagenesis. *J Biol Chem* **276**: 11902-11912
- Mettal U, Boland W, Beyer P, Kleinig H** (1988) Biosynthesis of Monoterpene Hydrocarbons by Isolated Chromoplasts from Daffodil Flowers. *European Journal of Biochemistry* **170**: 613-616
- Mignée C, Mutoh R, Krieger-Liszkay A, Kurisu G, Sétif P** (2017) Gallium ferredoxin as a tool to study the effects of ferredoxin binding to photosystem I without ferredoxin reduction. *Photosynth Res* **134**: 251-263
- Morigasaki S, Jin T, Wada K** (1993) Comparative studies on ferredoxin-NADP⁺ oxidoreductase isoenzymes derived from different organs by antibodies specific for the radish root- and leaf-enzymes. *Plant Physiol* **103**: 435-440
- Morigasaki S, Takata K, Suzuki T, Wada K** (1990) Purification and characterization of a ferredoxin-NADP⁺ oxidoreductase-like enzyme from radish root tissues. *Plant Physiol* **93**: 896-901
- Morstadt L, Graber P, de Pascalis L, Kleinig H, Speth V, Beyer P** (2002) Chemiosmotic ATP synthesis in photosynthetically inactive chromoplasts from *Narcissus pseudonarcissus* L. linked to a redox pathway potentially also involved in carotene desaturation. *Planta* **215**: 134-140
- Munekage Y, Hojo M, Meurer J, Endo T, Tasaka M, Shikanai T** (2002) PGR5 is involved in cyclic electron flow around photosystem I and is essential for photoprotection in *Arabidopsis*. *Cell* **110**: 361-371
- Mutoh R, Muraki N, Shinmura K, Kubota-Kawai H, Lee YH, Nowaczyk MM, Rogner M, Hase T, Ikegami T, Kurisu G** (2015) X-ray Structure and Nuclear Magnetic Resonance Analysis of the Interaction Sites of the Ga-Substituted Cyanobacterial Ferredoxin. *Biochemistry* **54**: 6052-6061
- Nivelstein V, Vandekerckhove J, Tadros MH, Lintig JV, Nitschke W, Beyer P** (1995) Carotene Desaturation Is Linked to A Respiratory Redox Pathway in *Narcissus-Pseudonarcissus* Chromoplast Membranes - Involvement of A 23-Kda Oxygen-Evolving-Complex-Like Protein. *European Journal of Biochemistry* **233**: 864-872

- O'Donnell VB, Tew DG, Jones OTG, England PJ** (1993) Studies on the Inhibitory Mechanism of Iodonium Compounds with Special Reference to Neutrophil Nadph Oxidase. *Biochemical Journal* **290**: 41-49
- Pateraki I, Renato M, Azcon-Bieto J, Boronat A** (2013) An ATP synthase harboring an atypical gamma-subunit is involved in ATP synthesis in tomato fruit chromoplasts. *Plant Journal* **74**: 74-85
- Peltier G, Aro EM, Shikanai T** (2016) NDH-1 and NDH-2 Plastoquinone Reductases in Oxygenic Photosynthesis. *Annual Review of Plant Biology* **67**: 55-80
- Peterman EJG, Wenk SO, Pullerits T, Palsson LO, Van Grondelle R, Dekker JP, Rogner M, Van Amerongen H** (1998) Fluorescence and absorption spectroscopy of the weakly fluorescent chlorophyll a in cytochrome b(6)f of *Synechocystis* PCC6803. *Biophysical Journal* **75**: 389-398
- Pierre Y, Breyton C, Lemoine Y, Robert B, Vernotte C, Popot JL** (1997) On the presence and role of a molecule of chlorophyll a in the cytochrome b(6)f complex. *Journal of Biological Chemistry* **272**: 21901-21908
- Prester T, Prochaska HJ, Talalay P** (1992) Inhibition of Nad(P)H-(Quinone Acceptor) Oxidoreductase by Cibacron Blue and Related Anthraquinone Dyes - A Structure Activity Study. *Biochemistry* **31**: 824-833
- Raorane ML, Narciso JO, Kohli A** (2016) Total Soluble Protein Extraction for Improved Proteomic Analysis of Transgenic Rice Plant Roots. *Methods in molecular biology* (Clifton, N J) **1385**: 139-147
- Reisinger V, Hertle AP, Ploescher M, Eichacker LA** (2008) Cytochrome b(6)f is a dimeric protochlorophyll a binding complex in etioplasts. *Febs Journal* **275**: 1018-1024
- Renato M, Boronat A, Azcon-Bieto J** (2015) Respiratory processes in non-photosynthetic plastids. *Frontiers in Plant Science* **6**: doi: 10.3389/fpls.2015.00496
- Renato M, Pateraki I, Boronat A, Azcon-Bieto J** (2014) Tomato Fruit Chromoplasts Behave as Respiratory Bioenergetic Organelles during Ripening. *Plant Physiology* **166**: 920-933
- Renné P, Dressen U, Hebbeker U, Hille D, Flugge UI, Westhoff P, Weber APM** (2003) The Arabidopsis mutant dct is deficient in the plastidic glutamate/malate translocator DiT2. *Plant Journal* **35**: 316-331
- Shinohara F, Kurisu G, Hanke G, Bowsher C, Hase T, Kimata-Arigo Y** (2017) Structural basis for the isotype-specific interactions of ferredoxin and ferredoxin: NADP+ oxidoreductase: an evolutionary switch between photosynthetic and heterotrophic assimilation. *Photosynthesis Research* **134**: 281-289
- Sirpiö S, Allahverdiyeva Y, Suorsa M, Paakkarinen V, Vainonen J, Battchikova N, Aro EM** (2007) TLP18.3, a novel thylakoid lumen protein regulating photosystem II repair cycle. *Biochemical Journal* **406**: 415-425

- Strand DD, Fisher N, Kramer DM** (2017) The higher plant plastid NAD(P)H dehydrogenase-like complex (NDH) is a high efficiency proton pump that increases ATP production by cyclic electron flow. *J Biol Chem.* **292**:11850-11860.
- Trebst A, Wietoska H, Draber W, Knops HJ** (1978) Inhibition of Photosynthetic Electron Flow in Chloroplasts by the Dinitrophenylether of Bromo-Nitrothymol Or Iodo-Nitrothymol. *Zeitschrift Fur Naturforschung C-A Journal Of Biosciences* **33**: 919-927
- Wagner AM, Krab K, Wagner MJ, Moore AL** (2008) Regulation of thermogenesis in flowering Araceae: The role of the alternative oxidase. *Biochimica et Biophysica Acta-Bioenergetics* **1777**: 993-1000
- Wang YQ, Yang Y, Fei Z, Yuan H, Fish T, Thannhauser TW, Mazourek M, Kochian LV, Wang X, Li L** (2013) Proteomic analysis of chromoplasts from six crop species reveals insights into chromoplast function and development. *Journal of Experimental Botany* **64**: 949-961
- Yamamoto H, Peng LW, Fukao Y, Shikanai T** (2011) An Src Homology 3 domain-like fold protein forms a ferredoxin binding site for the chloroplast NADH dehydrogenase-like complex in Arabidopsis. *Plant Cell* **23**: 1480-1493
- Zuo P, Li BX, Zhao XH, Wu YS, Ai XC, Zhang JP, Li LB, Kuang TY** (2006) Ultrafast carotenoid-to-chlorophyll singlet energy transfer in the cytochrome b(6)f complex from *Bryopsis corticulans*. *Biophysical Journal* **90**: 4145-4154

Table 1

O₂-consumption and alkalization of the medium by chromoplasts. (a) NADPH-dependent respiratory activity in chromoplasts was measured simultaneously with a pH and an oxygen electrode. The assay contained chromoplasts (300 µg protein ml⁻¹), 200 µM NADPH, 0.1 mM Tris/HCl pH 7.4, 10 mM MgCl₂. O₂-consumption in the absence of inhibitors was 8.1*10⁻⁸ ± 1.7 *10⁻⁸ mol O₂ min⁻¹ mg protein⁻¹) and the pH increased by 6.5*10⁻⁸ ± 1.8 *10⁻⁸ mol H⁺ min⁻¹ mg protein⁻¹). (b) NADPH- and NADH-dependent respiratory activity in chromoplasts. When 200 µM NADH instead of 200 µM NADPH is used, the respiratory activity is 6.1 *10⁻⁸ ± 1.1 *10⁻⁸ mol O₂ min⁻¹ mg protein⁻¹. Tables show mean values ±SD, n=3.

(a)

Sample	O ₂ -Consumption (%)	Alkalization (%)
No addition	100	100
20 µM DBMIB	23±5	84 ± 5
80 µM DNP-INT	25 ± 6	93 ± 8
0.5 µM Nigericin	95 ± 5	0
20 µM Octylgallate	0	0
0.5 µM Rotenone	75 ± 10	0

(b)

Sample	NADPH	NADH
No addition	100	100
50 µM DPI	10 ± 7	92 ± 5
20 µM Octylgallate	0	0
50 µM Cibacron	90 ± 4	32 ± 7
0.5 µM Rotenone	80 ± 10	0
1 mM KCN	100	100
20 µM DBMIB	23±5	100

Figure Legends

Fig. 1

NADPH-dependent respiratory activity in chromoplasts. Changes in pH and oxygen consumption were measured simultaneously. Representative traces are shown. The PTOX inhibitor octylgallate (OG; 20 μM) and the uncoupler nigericin (100 nM) were added as indicated by the arrows. The assay contained chromoplasts (300 μg protein ml^{-1}), 200 μM NADPH, 0.1 mM Tris/HCl pH 7.4, 10 mM MgCl_2 .

Fig. 2

Proteins of the respiratory chain of the chromoplast. Western blots were conducted with antibodies directed against the subunit H of the NDH complex (NDH-H), the plastid terminal oxidase (PTOX), the β subunit of the ATP-synthase (ATPb), cytochrome f (Cyt f), ferredoxin (Fd), ferredoxin-NADP oxidoreductase (FNR) and against the ferredoxin-plastoquinone reductase subunit of photosynthetic cyclic electron flow PGRL1. Total chromoplast protein loaded is indicated.

Fig. 3

Analysis of FNR and Fd isoforms in chromoplasts. A. Total (T), soluble (S) and membrane bound (M) chromoplast proteins were separated by SDS-PAGE (12%) and immunodetected first using a leaf-type FNR antibody followed by immunodetection using the root-type (arrowhead) FNR antibody. B. Chromoplast protein complexes were separated by BN gel electrophoresis, electroblotted and subjected to immunoblotting using leaf-type FNR antibody. C. Total proteins from leaf (L), root (R) and chromoplasts (C) of *Narcissus* plants were separated by SDS-PAGE (12%) and immunodetected with ferredoxin 3 (AtFd3, root-type), ferredoxin 1 (AtFd1, leaf-type) and TROL antibody. MW indicates the nearest molecular weight marker band.

Fig. 4

Inhibition of NADPH-dependent respiratory activity in chromoplasts by Ferredoxin-Ga (Fd-Ga). Black squares: increasing amounts of Fd-Ga inhibit chromorespiration; open squares: Fd-Fe (3.75 μM) restored the respiratory activity when added to samples inhibited 0.5, 0.7 and 1 μM Fd-Ga. The cross

denotes the addition of 10 μM DBMIB that did not result in further inhibition. The assay contained chromoplasts ($300 \mu\text{g protein ml}^{-1}$), 200 μM NADPH, 0.1 mM Tris/HCl pH 7.4, 10 mM MgCl_2 .

Fig. 5

Inhibition of NADPH-dependent respiratory activity in chromoplasts by inhibitors of the cytochrome *b₆f* complex and by Antimycin A. A, Inhibition by DBMIB; B, by DNP-INT; C, by Antimycin A. The cross in A denotes the addition of Fd-Ga that did not result in further inhibition. The assay contained chromoplasts ($300 \mu\text{g protein ml}^{-1}$), 200 μM NADPH, 0.1 mM Tris/HCl pH 7.4, 10 mM MgCl_2 .

Fig. 6

Difference absorption spectrum of chromoplasts. The difference of the spectra obtained in the presence of ferricyanide minus no addition is shown. The sample contained 0.5 mM 1,4-dithioerythritol. Addition of dithionite did not lead to further changes. OD at 450 nm (maximum absorption of the carotenoids) was 3. ΔA (-600 to +400) corresponds to approximately 1 mOD.

Fig. 7

Chlorophyll fluorescence spectra. Gray line, fluorescence of native chromoplasts in 100 mM Tris/HCl pH 7.4, 10 mM MgCl_2 ; black line, same chromoplast concentration extracted with acetone. The wavelengths of the fluorescence maxima are indicated. The fluorescence intensity obtained from native chromoplasts was multiplied by four. Inset: determination of the chlorophyll *a* content of chromoplasts. The fluorescence of the acetone extract of chromoplasts and of pure chl *a* solutions in acetone were measured to obtain a calibration curve.

Fig. 8

Model of the respiratory electron transport in chromoplasts. Two independent pathways reduce the plastoquinone pool which is oxidized by PTOX (yellow). In the first pathway electrons are

donated from NADPH via FNR, Fd to the cytochrome *b₆f*-dependent pathway which reduces PQ and does not lead to the formation of a proton gradient. In the second pathway (blue) NAD(P)H donates electrons to the NDH complex which reduces PQ and pumps protons fueling the ATP-Synthase. NADH serves as the main substrate for this pathway but NADPH functions also as substrate. Specific inhibitors of the different proteins/protein complexes are given in red.

Fig. 9

Model of electron transport via the cytochrome *b₆f* complex. PQ binds to the Q_i-site close to cyt *b_h* and cyt *c_i*. In a first reaction Fd_{red} donates an electron possibly via heme *ci* to the cyt *b_h* which reduces then PQ to PQ^{•-}. In a second step the next Fd_{red} reduces PQ^{•-} to PQH₂ which leaves the binding site. Both, the high potential chain and the Q-cycle are expected to be nonfunctional in the chromorespiratory pathway. The cofactors not participating in the electron transport are shown in gray. PGR5/PGRL1 as putative electron input module is omitted in this figure.

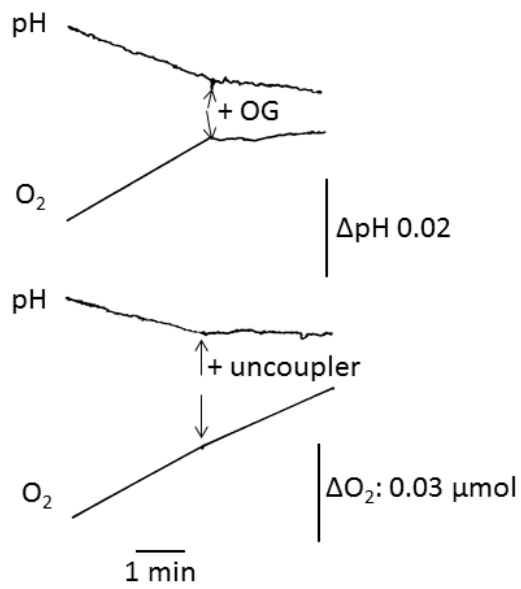
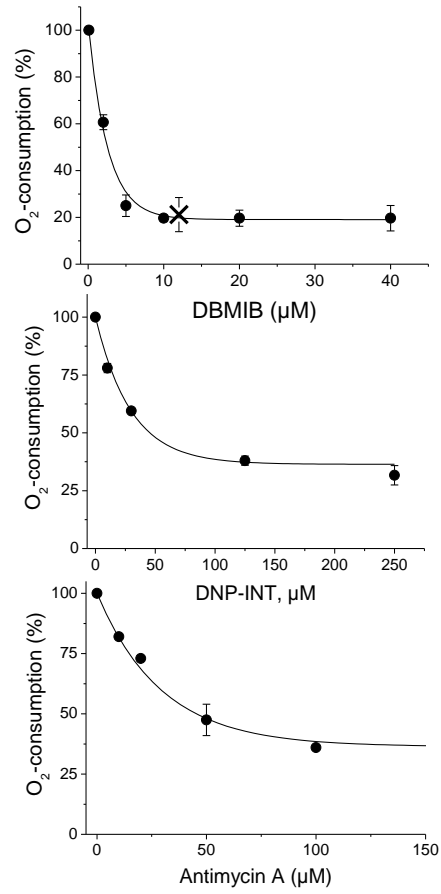


Fig. 1

NADPH-dependent respiratory activity in chromoplasts.

Changes in pH and oxygen consumption were measured simultaneously. Representative traces are shown. The PTOX inhibitor octylgallate (OG; 20 μM) and the uncoupler nigericin (100 nM) were added as indicated by the arrows. The assay contained chromoplasts (300 μg protein ml⁻¹), 200 μM NADPH, 0.1 mM Tris/HCl pH 7.4, 10 mM MgCl₂.



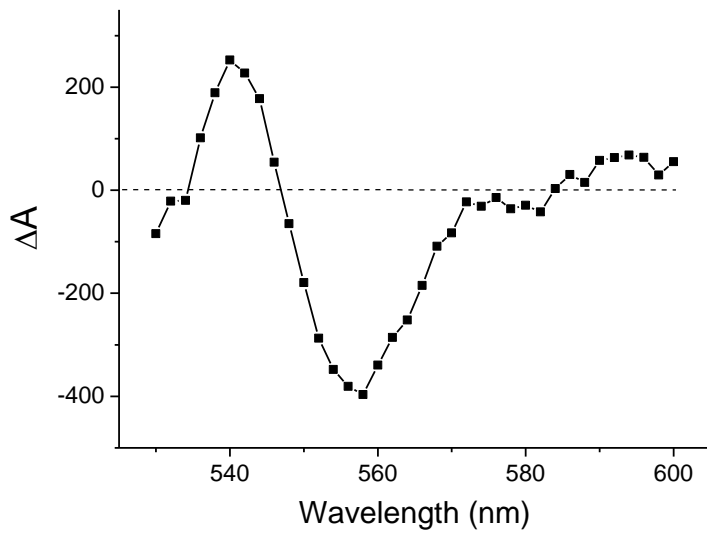


Fig. 6

Difference absorption spectrum of chromoplasts.

The difference of the spectra obtained in the presence of ferricyanide minus no addition is shown. The sample contained 0.5 mM 1,4-dithioerythritol. Addition of dithionite did not lead to further changes. OD at 450 nm (maximum absorption of the carotenoids) was 3. ΔA (-600 to +400) corresponds to approximately 1 mOD.

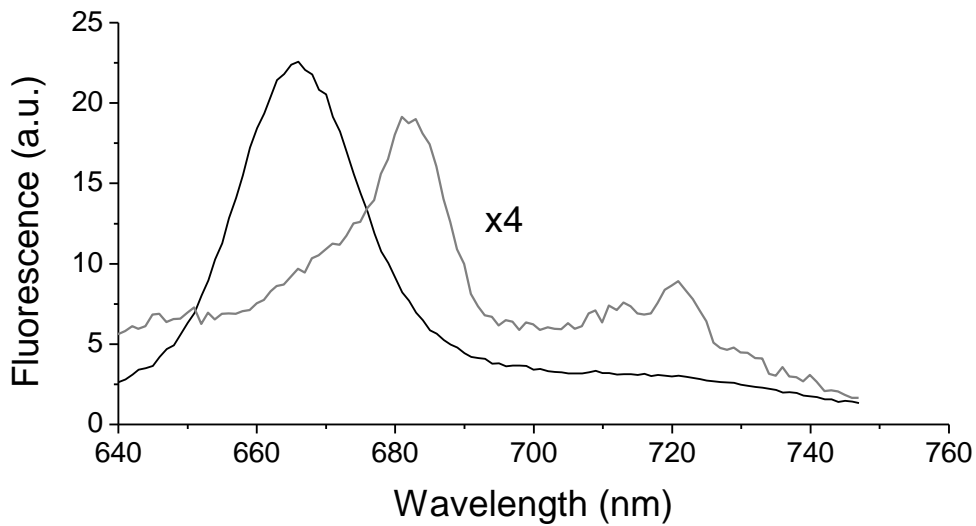


Fig. 7

Chlorophyll fluorescence spectra.

Gray line, fluorescence of native chromoplasts in 100 mM Tris/HCl pH 7.4, 10 mM $MgCl_2$; black line, same chromoplast concentration extracted with acetone. The wavelengths of the fluorescence maxima are indicated. The fluorescence intensity obtained from native chromoplasts was multiplied by four. Inset: determination of the chlorophyll *a* content of chromoplasts. The fluorescence of the acetone extract of chromoplasts and of pure chl *a* solutions in acetone were measured to obtain a calibration curve.

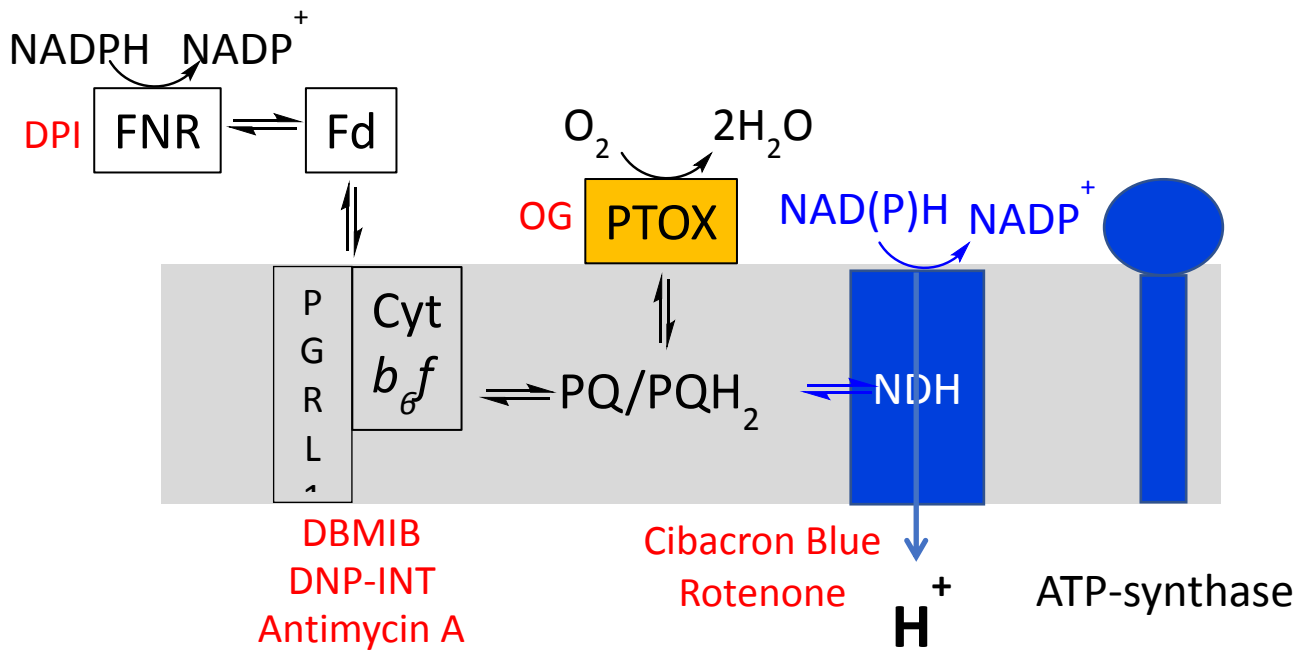


Fig. 8

Model of the respiratory electron transport in chloroplasts.

Two independent pathways reduce the plastoquinone pool which is oxidized by PTOX (yellow). In the first pathway electrons are donated from NADPH via FNR, Fd to the cytochrome *b₆f*-dependent pathway which reduces PQ and does not lead to the formation of a proton gradient. In the second pathway (blue) NAD(P)H donates electrons to the NDH complex which reduces PQ and pumps protons fueling the ATP-Synthase. NADH serves as the main substrate for this pathway but NADPH functions also as substrate. Specific inhibitors of the different proteins/protein complexes are given in red.

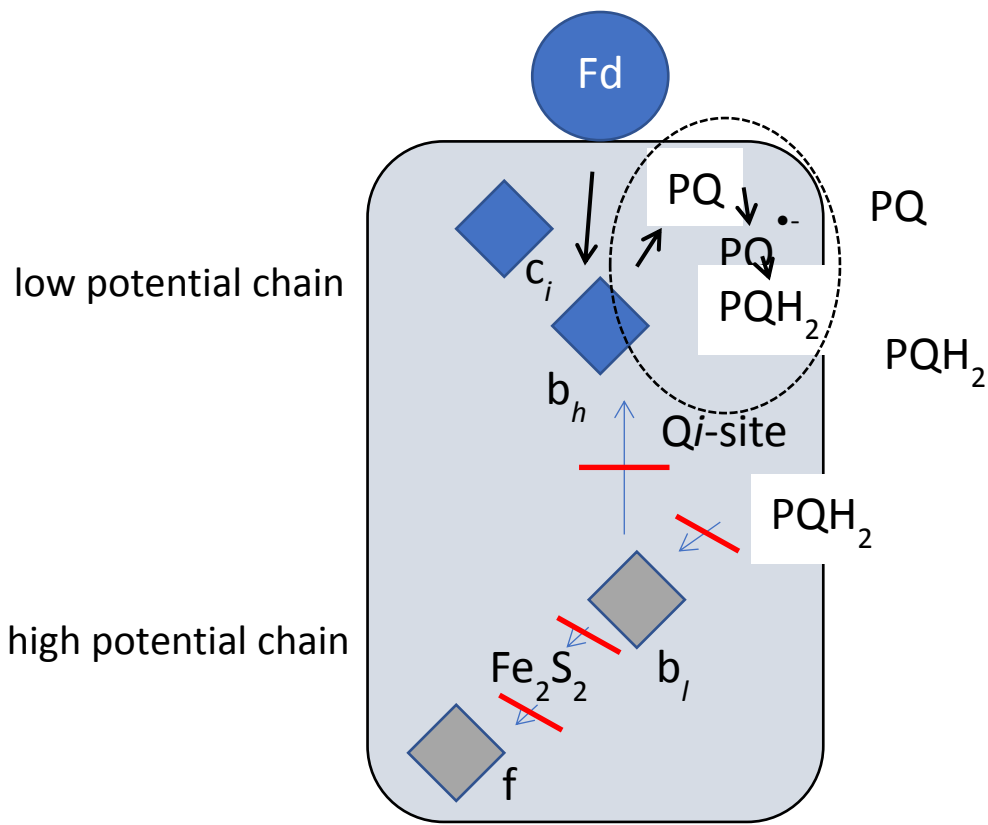
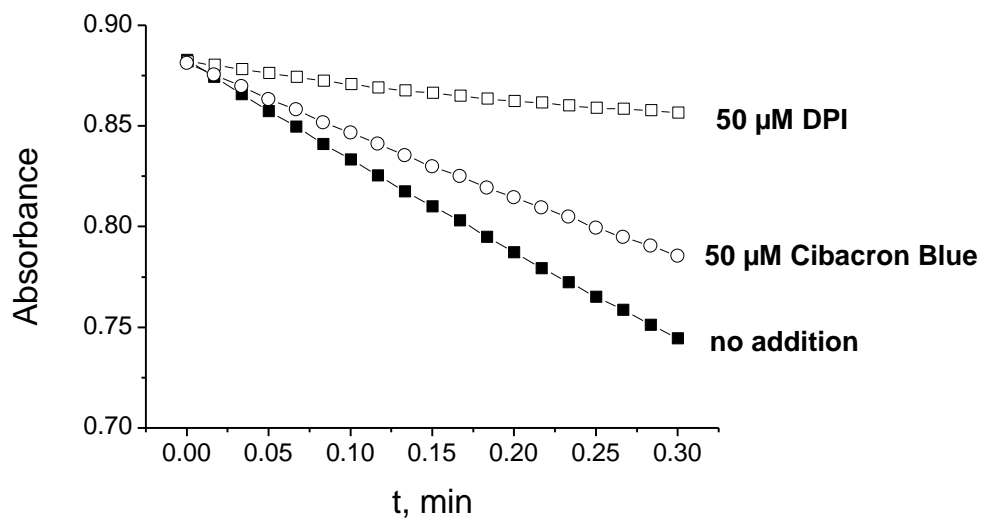


Fig. 9
Model of electron transport via the cytochrome b_6/f complex. PQ binds to the Q_i -site close to cyt b_h and cyt c_i . In a first reaction Fd_{red} donates an electron possibly via heme ci to the cyt b_h which reduces then PQ to $PQ^{\cdot-}$. In a second step the next Fd_{red} reduces $PQ^{\cdot-}$ to PQH_2 which leaves the binding site. Both, the high potential chain and the Q-cycle are expected to be nonfunctional in the chromorespiratory pathway. The cofactors not participating in the electron transport are shown in gray. PGR5/PGRL1 as putative electron input module is omitted in this figure.

Supplementary material

Fig. 1

Effect of DPI and Cibacron Blue on FNR-activity



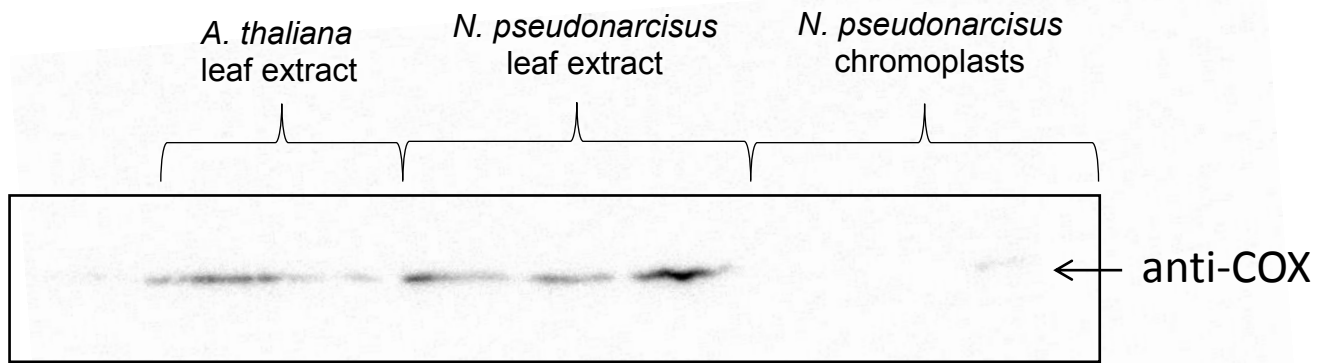
Diaphorase activity of FNR was measured as absorbance change at 600 nm. The assay contained 5 nM purified FNR from *Synechocystis* sp 6803, 20 μM 2,6-dichlorophenolindophenol (DCPIP), 33 μM NADPH, 50 mM NaCl, 20 mM Tris, pH 8.0. When indicated, FNR was preincubated for 1 min in the presence of diphenylene iodonium (DPI) or cibacron Blue 3G-A before addition of NADPH, DCPIP.

Supplementary material

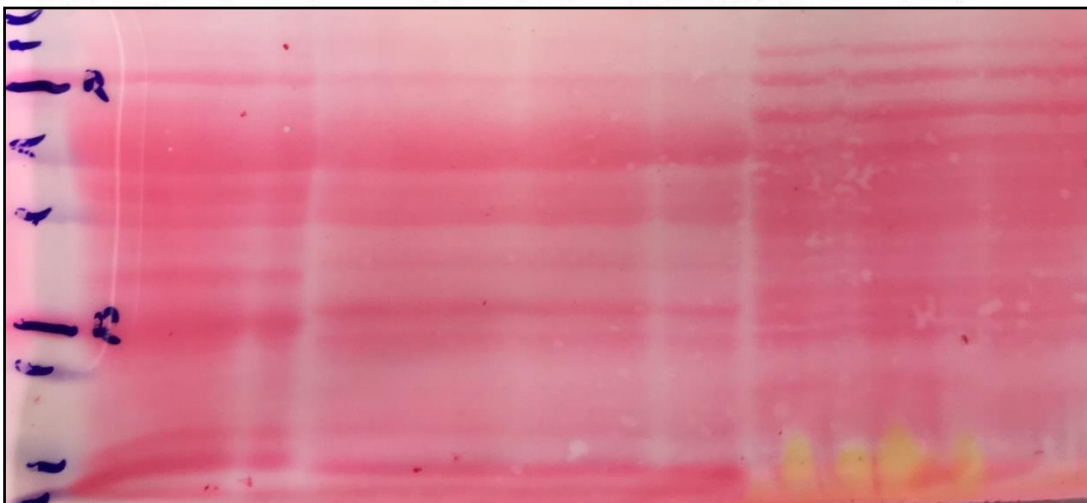
Fig. 2

Probing for contamination of the chromoplast preparation with mitochondria

Immunoblot,



Nitrocellulose membrane, Poinceau staining



Leaf extracts from *A. thaliana* and *N. pseudonarcissus* were obtained by crushing the leaves in liquid nitrogen. Leaf powder was resuspended in a buffer containing 0.3 M sorbitol, 1 mM MgCl₂, 10 mM EDTA, 50 mM KCl, 20 mM HEPES pH 7.6. For *A.*

thaliana 15 µl and 5 µl, for *N. pseudonarcissus* 40 µl, 20 µl and 10 µl leaf extract, for chromoplasts 10 µl, 20 µl and 40 µl were loaded on a 12% SDS-PAGE.

Supplementary material

Table 1

O₂-consumption by chromoplasts. Effect of myxothiazol and amino-NADH

NADH-dependent respiratory activity in chromoplasts was measured with an oxygen electrode. The assay contained chromoplasts (300 µg protein ml⁻¹), 200 µM substrate, 0.1 mM Tris/HCl pH 7.4, 10 mM MgCl₂. O₂-consumption with NADH was $6.1 \cdot 10^{-8} \pm 1.1 \cdot 10^{-8}$ mol O₂ min⁻¹ mg protein⁻¹. Table shows mean values ±SD, n=3.

sample	O₂-consumption (mol O ₂ min ⁻¹ mg protein ⁻¹)
NADH	$6.1 \cdot 10^{-8} \pm 1.1 \cdot 10^{-8}$
amino-NADH	$7.1 \cdot 10^{-8} \pm 0.8 \cdot 10^{-8}$
NADPH + 25 µM myxothiazol	$6.9 \cdot 10^{-8} \pm 1.7 \cdot 10^{-8}$
NADH + 25 µM myxothiazol	$6.3 \cdot 10^{-8} \pm 1.0 \cdot 10^{-8}$